JOURNAL OF APPLIED ELECTROCHEMISTRY 23 (1993) 1285–1292

A modified Hull cell with forced electrolyte flow: simulation of industrial electroplating conditions

M. DEGREZ, A DUCHÊNE, A. FONTANA, R. WINAND

Université Libre de Bruxelles, Department of Metallurgy–Electrochemistry, CP 165, Avenue F.D. Roosevelt, 50, B 1050 Brussels, Belgium

Received 9 March 1992; revised 14 January 1993

Hull cells are often used to determine the optimum current density range for industrial electroplating. However, these cells do not reproduce correctly the hydrodynamic conditions. The design and the use of a modified Hull cell able to reproduce constant hydrodynamic conditions at the cathode for a large range of circulation speeds are described. Mass transfer and current distribution at the cathode have been evaluated in this cell for copper and zinc deposition.

1. Introduction

The structure and properties of electrodeposits depend on several parameters. Two of these play a major role in electrocrystallization and structure determination: mass transfer, represented by the ratio of the current density, j, to the diffusion limiting current density, j_{dl}, and the inhibition effects due to the presence at the electrode surface of substances different from the depositing metal which are physically or chemically adsorbed.

For industrial purposes, plating tests are used for predictive quality control. The Hull cell, eventually modified, is widely used because it covers a wide current density range using a single cathode. Several cathodes are prepared for all the important bath variables and serve as control references.

An important disadvantage of all existing Hull cells is that industrial hydrodynamic conditions are not reproduced correctly in these cells; variations in the ratio j/j_{dl} along the height of the cathode imply that the results cannot be directly transferred to the plant.

The aim of this work was to design and to build a modified Hull cell able to reproduce constant hydrodynamic conditions at the cathode and to simulate modern types of industrial cells where mass transfer is improved by electrolyte flow parallel to the electrodes.

It is difficult to combine a wide variation in current densities and constant hydrodynamic conditions at the cathode. This last criterion is the most important making use of the cell to prospect new industrial electroplating conditions. The choice of the cross section of the cell was thus based on this preferential criterion.

This modified Hull cell was characterized for copper electrowinning and electrorefining and for zinc electrowinning. Using tracer methods, mass transfer at the cathode was evaluated in order to check the hydrodynamic homogeneity of the cell. Furthermore, the current distribution on the cathode for each electrochemical system was modelled, thus allowing for easy and accurate determination of the real current density corresponding to given deposit properties.

2. Theoretical considerations

Metal distribution in electroplating is very important, regardless of the purpose of the plating operation.

The distribution of an electrodeposit on a substrate is determined by the local current density at each point and by the cathodic current efficiency at that current density. The local current density in turn is determined by the primary current distribution and the local polarization. The primary current distribution is determined completely by the geometry of the plating cell. It is independent of the properties of the solution provided they are uniform, right up to the electrode surface. The distortion of the primary current distribution by polarization and other factors at the electrode results in the secondary current distribution [1].

The secondary current distribution is always more uniform than the primary distribution, provided the slope of the polarization curve is not negative. It should also be noted that the polarization and conductivity are not inherent properties of the solution alone, but depend on other factors such as temperature, agitation and current density. Poor mass transfer can also alter the conductivity of the solution in the vicinity of the cathode but this effect is small.

Using the dimensionless Wagner number, defined as

$$Wa = \frac{d\eta}{dj}\left(\frac{\kappa}{L}\right) \quad (1)$$

where κ is the solution conductivity, L is a characteristic geometric length (here the difference between the maximum and the minimum anode to cathode distance) and $d\eta/dj$ is the slope of the potential–

0021-891X

current curve, Ibl [2] quantifies the uniformity of the current distribution. The latter is more uniform the larger the Wagner number. At high current densities, if Tafel's law holds, the slope $d\eta/dj$ is inversely proportional to j so that Wa decreases with increasing current density.

In the conventional Hull cell, the following relationship between the primary current density (j_{prim}) and the dimensionless cathode length, measured from the lower end (χ), is still in use today [3]:

$$j_{prim} = j_{mean}[2.33 \log_{10}(1/(1-\chi)) - 0.08] \quad (2)$$

where j_{mean} is the average current density. The generalized form of this relation is [5, 6]:

$$j_{prim} = j_{mean}(a - b \log_{10} x) \quad (3)$$

where x is the distance along the cathode measured from the end nearest to the anode. With the finite element method and the boundary element method, Matlosz *et al.* [4] have extensively studied the secondary current distribution in the Hull cell in the absence of mass transfer effects and without variation of the anodic overvoltage. However, due to edge effects and to non-uniform mass transfer at the cathode, the local current density is known with a good approximation only in the central zone of the cathode [5–7].

Terakado and Nagasaka [8] have proposed a modified Hull cell with symetrical electrodes, which we call the TENA cell in this paper for convenience, giving a simple analytical solution for the primary current distribution. Figure 1 shows a cross section of such a cell where the two electrodes have the same length, in contrast to those in the Hull cell, and are located on the radius of two concentric circles. Whatever the value of the angle α, the four angles of the cell are right. Owing to the arc shape of the current lines, the primary current density at any point on the cathode is given by

$$j_{prim}(x') = \frac{I_T}{h \ln(b/a)}\left(\frac{1}{x'}\right) \quad (4)$$

where I_T is the total current, h the height of the electrode and x' the distance from the centre of the circles along the cathode, with a and b, respectively, the minimum and the maximum of its value.

In this paper, the TENA cell was modified to ensure uniform mass transfer to the electrode by flowing the electrolyte through the cell parallel to the electrodes.

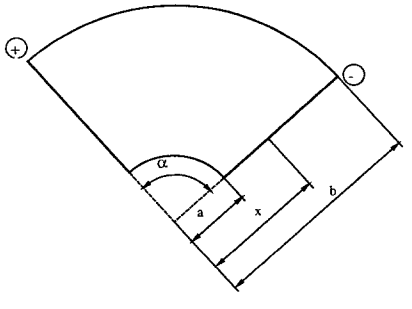

Fig. 1. Cross section of a TENA cell [8].

It should be noted that the electrodes do not fully occupy their respective sides of the cell due to their finite height. Newman *et al.* [9–12] developed a model for this and showed that the primary current density is reasonably uniform over a substantial part of the electrode apart from the infinite current densities predicted at the upstream and downstream ends of the electrode. The effect of polarization reduces locally high current densities and makes the secondary current distribution more uniform, especially at the downstream end of the cathode.

To test the uniformity of mass transfer to the cathode, it is necessary to measure it. One of the best methods to characterize mass transfer is the tracer method, described in a previous paper [13], of which the basic principle is as follows. A small concentration of a soluble tracer ion is added to the electrolyte which must plate at a more positive potential than the studied metal and be deposited at the cathode at its own diffusion limiting current density, $j_{dl\ tracer}$, during the deposition of the studied metal Me. Chemical analysis gives the mass of tracer in the deposit and thus $j_{dl\ tracer}$ can be calculated. As a function of the hydrodynamic conditions (fully developed or developing flow, laminar or turbulent), the diffusion limiting current density of the metal, $j_{dl\ Me}$, can be then estimated.

During non-noble metal deposition, for example zinc deposition, there is coreduction of H^+. Hydrogen evolution enhances mass transfer owing to the intense local agitation in the diffusion layer due to gas bubbling through it. For hydrodynamically controlled mass transfer with a gas evolution contribution, it was proposed [14, 15, 19] to calculate the total $j_{dl\text{-}Me}$ by the addition of two independent factors: one, $j_{dl\text{-}Me\text{-}v}$, is due to macroconvection (forced flow of the electrolyte) and proportional to $v^{0.8}$ or $v^{-0.5}$ (turbulent or laminar flow), and the other, $j_{dl\text{-}Me\text{-}g}$, is due to microconvection and proportional to the square root of the volume of gas produced at the electrode or, better, to the square root of the partial current density j_{H2}.

3. Experimental procedure

The electrolytic cell, made of polyacrylate, was designed like a TENA cell but was provided with a flow of electrolyte parallel to the electrode surface. Figure 2 shows a cross section of the cell; by reference to Fig. 1, the electrolytic channel was designed with $\alpha = 19.2°$, $a = 3$ cm and $b = 12$ cm, but with a trapezoidal shape. Therefore, instead of four right angles, the cell cross section shows two acute angles of 80.4° and two obtuse angles of 99.6°.

The electrolyte circuit (Fig. 3) comprises a 100 litre electrolyte tank (T), two centrifugal pumps (P1 and P2), a flowmeter (F), the electrolysis cell (C) and a 50 cm long adaptative channel (A) to pass from the circular section of the pipes to the trapezoidal section of the cell and to ensure a fully developed flow in the cell. Conditions to ensure the

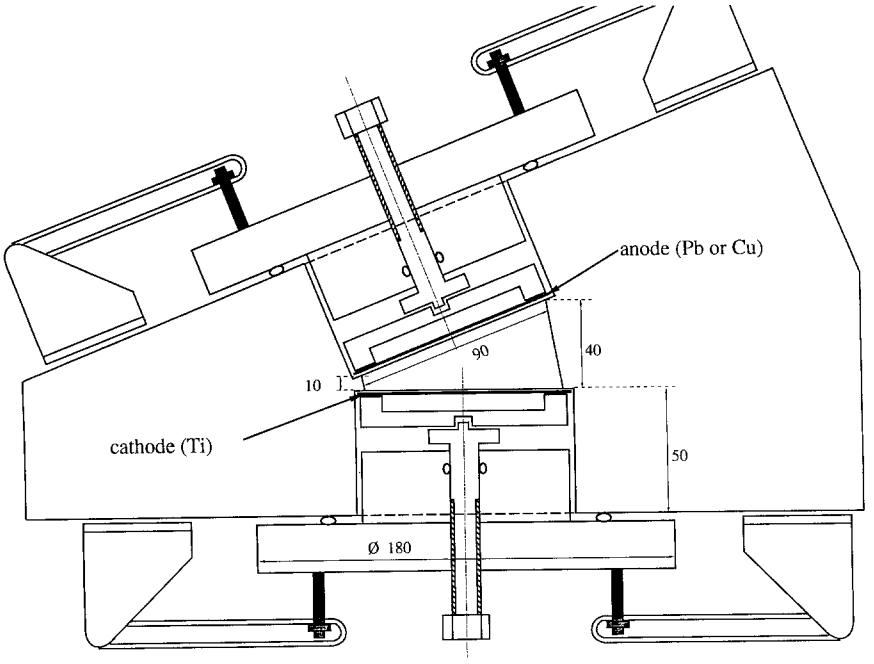

Fig. 2. Cross section of the modified Hull cell used in this paper.

hydrodynamic homogeneity in a trapezoidal shape section are not described in the literature. At this stage of the research, a small value of the α angle was chosen in order to keep a more or less rectangular section.

An electrical circuit included a 10 A–30 V d.c. power supply, a timer, an ammeter, a current integrator and a voltmeter for the anode-to-cathode voltage drop. Current was fed to the electrodes by pressure contacts on their reverse side.

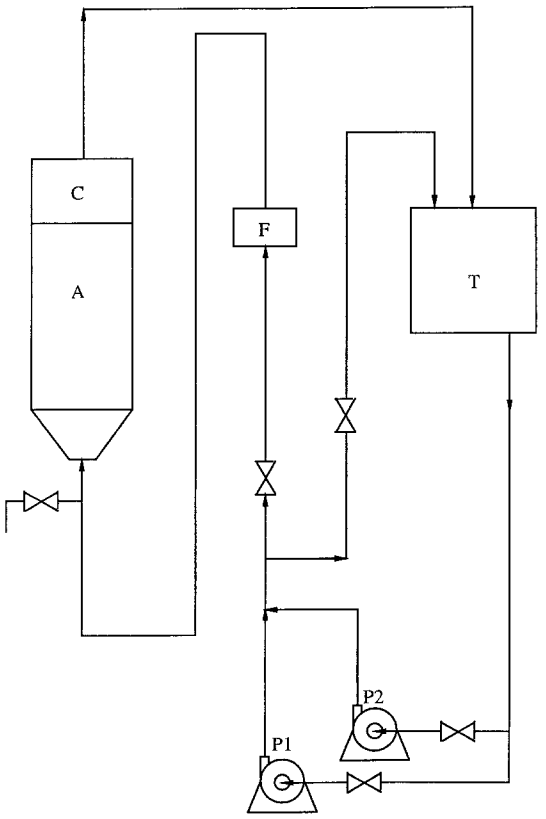

Fig. 3. Electrolyte circuit. (c) electrolysis cell; (A) adaptive channel; (F) flowmeter; (T) electrolyte tank; (P1) and (P2) centrifugal pumps.

The cathode was a polished titanium sheet. The anode was a pure lead sheet for electrowinning and a copper sheet for copper electrorefining. Both anode and cathode had an active area of 45 cm^2 (5 cm high and 9 cm long).

Analytical quality products were used to prepare the electrolyte solutions. The first was an acid copper sulphate bath (190 g dm^{-3} H_2SO_4, 50 g dm^{-3} Cu^{2+}, 1 mg dm^{-3} Ag^+ as tracer) and the second an acid zinc sulphate bath (100 g dm^{-3} H_2SO_4, 50 g dm^{-3} Zn^{2+}, 10 g dm^{-3} Cd^{2+} as tracer). The solutions were kept at 25° C.

Copper and zinc deposits were obtained at constant current ranging from 0.5 to 10 A for a quantity of electricity of 14 400 C (4 A h). The electrolyte velocity was in the range 0.15 to 1.5 m s^{-1}.

After electrolysis, the deposits were stripped off the titanium blanks, weighed and cut to give a number of samples. These samples were also weighed and their silver or cadmium content was determined by atomic absorption spectrometry after complete dissolution in nitric acid for copper samples, or hydrochloric acid for zinc samples.

To estimate the secondary current distribution, polarization curves were plotted in a separate cell in the copper sulphate bath using a potentiostat, a saturated sulphate reference electrode and a Pt counter-electrode. The working electrode was a Pt rotating disc electrode (r.d.e.) with a copper predeposit for cathodic copper deposition and anodic copper dissolution polarization curves, and a stationary lead electrode for the anodic oxygen evolution polarization curve. Ohmic drop was determined by a pulse method. The polarization curves were stored in a data bank or approximated by an analytical function valid over a particular range of current density.

4. Results and discussion

4.1. *Mass transfer to the cathode*

4.1.1. Copper deposition. Copper deposition from an acid sulphate bath occurs without hydrogen evolution. Accordingly, mass transfer to the cathode characterizes hydrodynamic conditions established by the flow of electrolyte through the cell.

Measurements were made during copper electrorefining at a current of 1 A using silver as the tracer. According to the theory [13], the diffusion limiting current density of copper can be calculated by:

$$j_{\mathrm{dl\,Cu^{2+}}} = j_{\mathrm{dl\,Ag^{+}}} \frac{[\mathrm{Cu^{2+}}]}{[\mathrm{Ag^{+}}]} \left(\frac{D_{\mathrm{Cu^{2+}}}}{D_{\mathrm{Ag^{+}}}}\right)^{2/3} \quad (5)$$

with $[\mathrm{Cu^{2+}}] = 787\,\mathrm{mol\,m^{-3}}$, $[\mathrm{Ag^{+}}] = 9.27 \times 10^{-3}\,\mathrm{mol\,m^{-3}}$ and $D_{\mathrm{Cu^{2+}}}/D_{\mathrm{Ag^{+}}} = 0.67$ [13, 16].

Four reproducible deposits were made at an electrolyte velocity of $0.2\,\mathrm{m\,s^{-1}}$. Each was cut into 36 samples of $1 \times 1.25\,\mathrm{cm^2}$ which were chemically analysed. A mapping of the mass transfer at the cathode was thus obtained.

Curve a in Fig. 4 gives $j_{\mathrm{dl\,Cu^{2+}}}$ as a function of the height along the cathode in the flow direction. The results illustrate the effect of the hydrodynamic entrance length [17]: the mass transfer is enhanced at the entrance of the cell. Nevertheless, the results show that a fully developed flow and a constant concentration boundary layer are achieved over about 80% of the electrode, downstream. Further results described below are based only on this downstream part of the cathode.

Mass transfer distribution along the length of the cathode is given by curve b in Fig. 4 at an electrolyte velocity of $0.2\,\mathrm{m\,s^{-1}}$. The anode-to-cathode distance is 1 cm at $x = 0$ and 4 cm at $x = 9$ cm (Fig. 2). The mass transfer is homogeneous with a maximum deviation *versus* the mean value of 5.7%.

An increase of the electrolyte velocity gives a more uniform mass transfer distribution with a slight decrease in the narrow space of the cell ($x < 2$ cm).

It is interesting to observe that the mass transfer on the 80% downstream part of the cathode in the case of copper deposition (thus without gas evolution) is controlled by a fully developed turbulent flow. Here, the only parameter is the speed of electrolyte (v). The Chilton–Colburn equation [13, 18]

$$Sh \propto Re^{0.8} \times Sc^{1/3} \quad (6)$$

is thus reduced to

$$j_{\mathrm{dl\,Cu^{2+}}} \propto v^{0.8} \quad (7)$$

Figure 5 shows that the law is verified and that turbulent flow is achieved in this cell even at less than $0.2\,\mathrm{m\,s^{-1}}$. This is due to the special shape of the cell cross section.

4.1.2. Zinc deposition. Current efficiency for zinc deposition is always less than 100%, since during the electrolysis hydrogen evolution occurs at the cathode. This enhances mass transfer even under turbulent flow conditions [13]. These experiments permit determination of the limits of the use of this cell in constant mass transfer conditions, in the case of non-noble metal deposition.

Measurements were performed during zinc electrowinning at an electrolyte velocity of $0.35\,\mathrm{m\,s^{-1}}$ and two total currents, 1 A and 4 A, using cadmium as the tracer. In this solution, due to the lack of knowledge of the value of the diffusion coefficients, the diffusion limiting current density of zinc can be estimated by:

$$j_{\mathrm{dl\,Zn^{2+}}} = j_{\mathrm{dl\,Cd^{2+}}} \cdot \frac{[\mathrm{Zn^{2+}}]}{[\mathrm{Cd^{2+}}]} \times 1 \quad (8)$$

with $[\mathrm{Zn^{2+}}] = 765\,\mathrm{mol\,m^{-3}}$ and $[\mathrm{Cd^{2+}}] = 8.9 \times 10^{-2}\,\mathrm{mol\,m^{-3}}$.

The deposits at 1 A were obtained with a mean current efficiency of 86%. Mass transfer along the length of the cathode, given by curve a in Fig. 6, remains constant with a maximum variation of 3.2%. At this total current, the partial current density for hydrogen is proportionally low.

The influence of hydrogen evolution appears in a more striking way in the case of zinc deposition at 4 A; the deposits were obtained with a mean current efficiency of 90%. Curve b in Fig. 6 shows that the mean mass transfer is enhanced by gas evolution

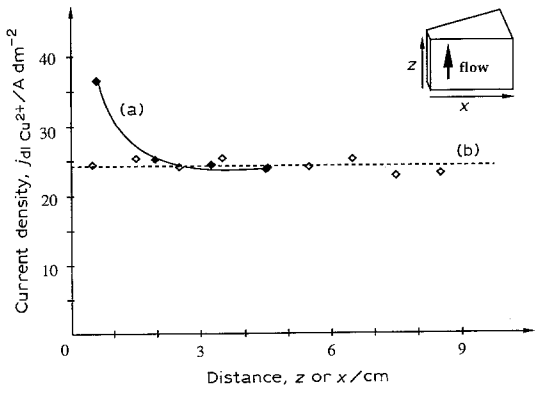

Fig. 4. Copper mass transfer: $v = 0.2\,\mathrm{m\,s^{-1}}$. (a) along the height of the cathode; (b) along the length of the cathode.

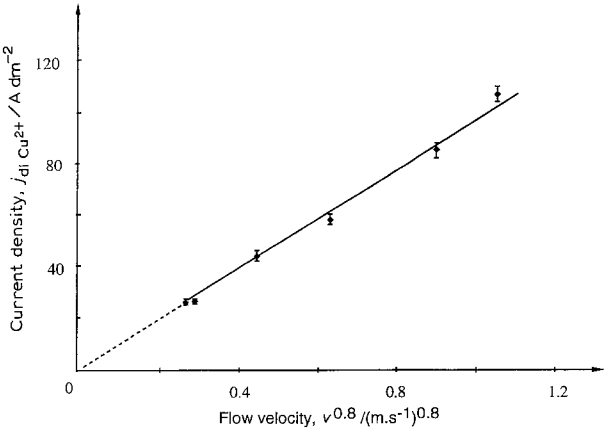

Fig. 5. Validity of Chilton–Colburn equation for copper mass transfer.

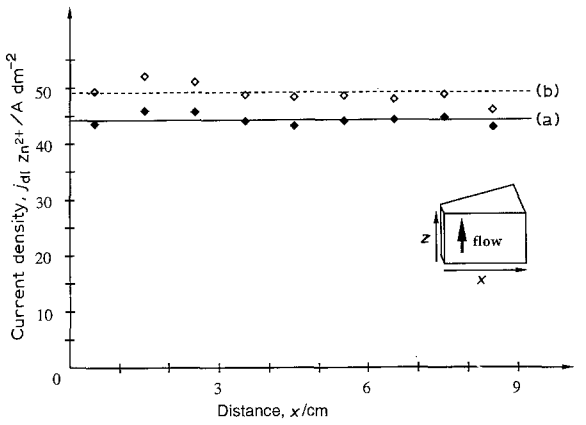

Fig. 6. Zinc mass transfer along the length of the cathode. (a) $v = 0.35\,m\,s^{-1}$, $I_{tot} = 1\,A$; (b) $v = 0.35\,m\,s^{-1}$, $I_{tot} = 4\,A$.

($j_{dl\,Zn^{2+}}$ increases from 44 to 49 A dm^{-2} when I_{total} changes from 1 A to 4 A) and that its distribution is less uniform with upper values in the narrow space of the cell where the local current density is higher. Nevertheless, the variation remains smaller than 7%.

It can be concluded from this paragraph that, in spite of the trapezoidal shape of the cross section, the flow through the modified Hull cell provides satisfactory homogeneous mass transfer on most of the cathode surface even if hydrogen evolution occurs during metal deposition.

However, in this latter case, Fig. 6 shows that the mass transfer values at both ends of the cathode are systematically lower than the expected values. This experimental fact cannot be explained at present; there may be a wall effect in the cell.

4.2. *Metal distribution on the cathode*

To predict the exact local amount of metal deposited, secondary current distribution and local current efficiency must be simultaneously known. Below, it is explained why this is very difficult to achieve in the case of zinc deposition from an acid sulphate bath.

With the cell cross section shown in Fig. 2 with a ratio $b/a = 4$ and 5 cm high electrodes, Equation 4, where $x' = x + a$, gives an analytical primary current distribution:

$$j_{prim}(x) = \frac{I_T}{5 \ln 4}\left(\frac{1}{x+3}\right) \qquad (9)$$

with x the distance (in cm) along the length of the cathode and $a = 3$ cm the distance from the center of the circles to the beginning of the cathode. This gives a value of $j_{max}/j_{min} = 4$.

Figure 2 shows that lateral walls of the cell are not circular but linear; this means that the current lines at both ends of the cathode are not arcs but chords. Nevertheless, due to the low value of the angle α, the ratio between the arc length and the chord length is 1.0047; the influence of the linear lateral walls on the variation *versus* the primary current distribution at these ends is thus very weak.

4.2.1. Copper deposition. A mapping of the copper distribution on the cathode was obtained in the same way as already described for the mass transfer experiments.

The first measurements confirm Newman's theory [9–12] cited in the theoretical part. Metal distribution along the height of the cathode increases at the outlet of the cell and even more at the inlet. However, after removal of 20% of the deposit surface (equivalent to 6 mm in the upstream and 4 mm in the downstream part of the deposit), about 70 wt % of the deposit remains with a very constant distribution along the height of the cathode. For this useful part of the deposit, the primary current distribution can be calculated according to

$$j_{prim}(x) = \frac{I_{useful}}{4 \ln 4}\left(\frac{1}{x+3}\right) \qquad (10)$$

where I_{useful} is the current determined by the weight of this part of the deposit.

The results obtained from the analysis of the deposits described below are always based on this method. All the copper deposits were obtained with a total current efficiency greater than 98%.

From the polarization curves, the secondary current distribution may be predicted using a simple model where, by assumption, the current lines are not modified by polarization (it can be shown that with the electrochemical system studied here, the maximum modification of the current lines is about 0.2%). This means that, due to the geometry of the TENA cell, the anodic and cathodic current densities are equal for the same x value. The first step is to plot the cathodic and anodic polarization curves, corrected for the ohmic drop. The difference between the two curves gives the anode to cathode galvanic potential of the system ($U_{gA/C}$) and is approximated by an analytical function in the useful range of current density. Cell voltage ($U_{A/C}$) and solution resistivity (ρ) must also be known.

The secondary current distribution at any x value is then estimated step by step by iteration:

(i) a first approximation of the secondary current

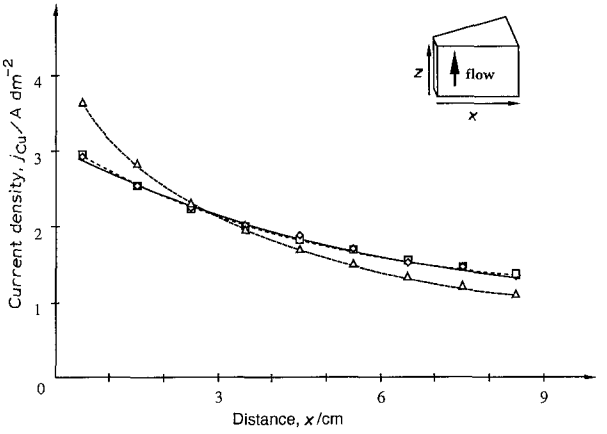

Fig. 7. Copper distribution (j_{exp}, ◇), primary (j_{prim}, △), and secondary (j_{sec}, □), current distributions along the length of the cathode. Copper electrorefining; $v = 0.2\,m\,s^{-1}$; $j_{mean} = 1.96\,A\,dm^{-2}$.

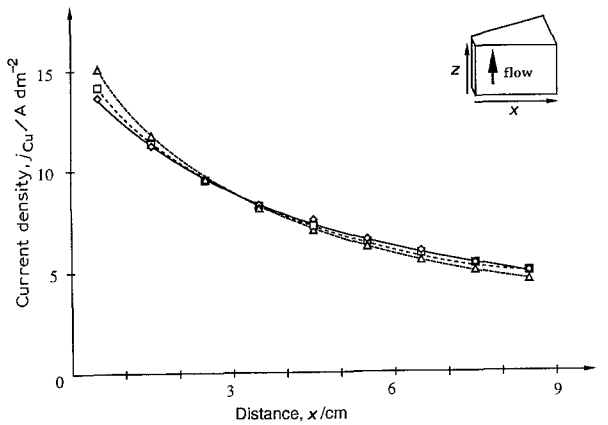

Fig. 8. Copper distribution (j_{exp}, ◇), primary (j_{prim}, △), and secondary (j_{sec}, □), current distributions along the length of the cathode copper electrorefining; $v = 0.2\,m\,s^{-1}$; $j_{mean} = 8.1\,A\,dm^{-2}$.

density $j_{sec}(x)$ is calculated by

$$j_1(x) = \frac{U_{A/C}}{\rho\alpha(x+3)} \tag{11}$$

(ii) $U_{gA/C}(j_1(x))$ is deduced

(iii) a second approximation of $j_{sec}(x)$ is given by

$$j_2(x) = \frac{U_{A/C} - U_{gA/C}(j_1(x))}{\rho\alpha(x+3)} \tag{12}$$

(iv) and so on until the difference

$$U_{A/C} - (U_{gA/C}(j(x)) + \rho\alpha(x+3)\,j(x)) \tag{13}$$

is less than 0.1 mV.

Figures 7 to 11 show experimental copper distribution (j_{exp}) along the length of the cathode obtained under different electrolysis conditions and also the calculated primary and secondary current distributions. Values are given at the mean x value of each sample. It is thus not surprising that the ratio of the maximum (at $x = 0.5$) to the minimum (at $x = 8.5$) primary current densities is 3.3 instead of the expected value of 4 based on the b/a ratio. Experimentally, this ratio ranges from 2.1 to 3, with respect to the polarization effect.

The results are now described in more detail.

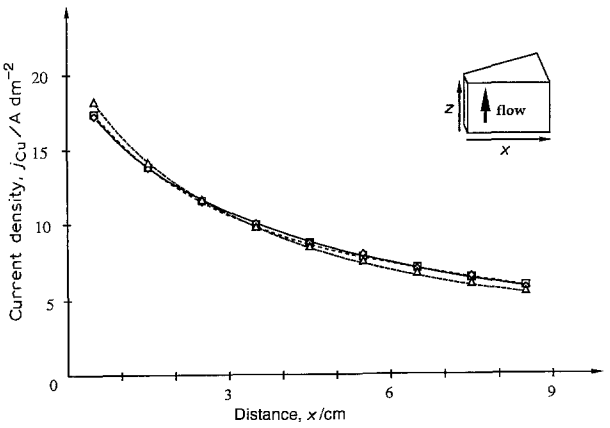

Fig. 9. Copper distribution (j_{exp}, ◇), primary (j_{prim}, △), and secondary (j_{sec}, □), current distributions along the length of the cathode copper electrorefining; $v = 0.7\,m\,s^{-1}$; $j_{mean} = 9.8\,A\,dm^{-2}$.

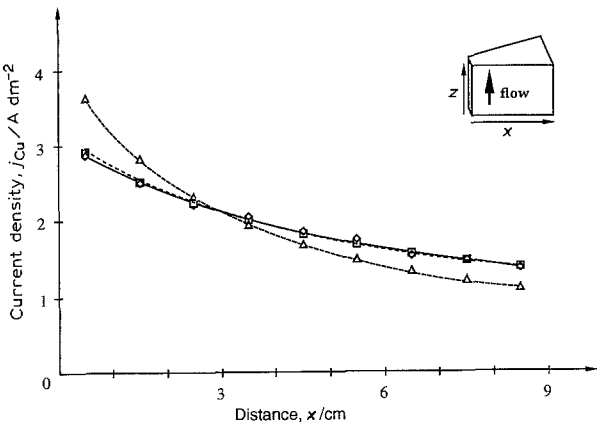

Fig. 10. Copper distribution (j_{exp}, ◇), primary (j_{prim}, △), and secondary (j_{sec}, □), current distributions along the length of the cathode copper electrowinning; $v = 0.35\,m\,s^{-1}$; $j_{mean} = 1.96\,A\,dm^{-2}$.

(a) *Copper electrorefining*

In this case, the cathodic and the anodic reactions are in opposite directions: copper reduction and dissolution. Thus the anode to cathode reversible potential is zero. Figure 12 gives the anode to cathode polarization curve. The secondary current distribution becomes significantly different from the primary when the total overvoltage is high compared to the ohmic drop. This is only the case when the current density is low. Furthermore, due to the high current efficiency, metal distribution and secondary current distribution are similar. This has been qualitatively verified by experiments. The copper distribution obtained at low mean current density (Fig. 7) differs to a greater extent from the primary current distribution than that obtained at high mean current density (Fig. 8), under the same other conditions.

The following will illustrate the model used to estimate the secondary current distribution.

Example 1: Copper electrorefining at an electrolyte velocity of $0.2\,m\,s^{-1}$, low mean current density ($1.96\,A\,dm^{-2}$) and low value of j/j_{dl} (Fig. 7).

The following data are used for calculation: cell

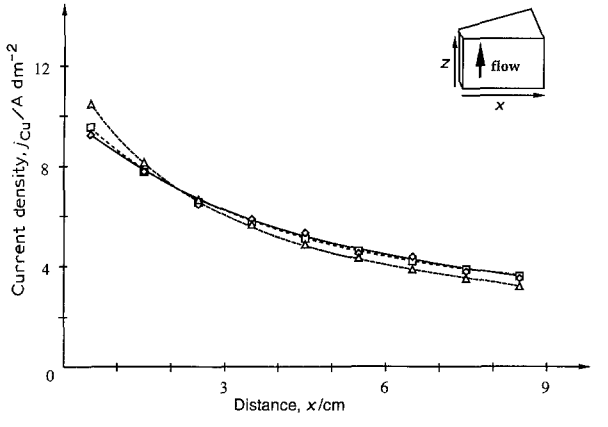

Fig. 11. Copper distribution (j_{exp}, ◇), primary (j_{prim}, △), and secondary (j_{sec}, □), current distributions along the length of the cathode copper electrowinning; $v = 0.35\,m\,s^{-1}$; $j_{mean} = 5.65\,A\,dm^{-2}$.

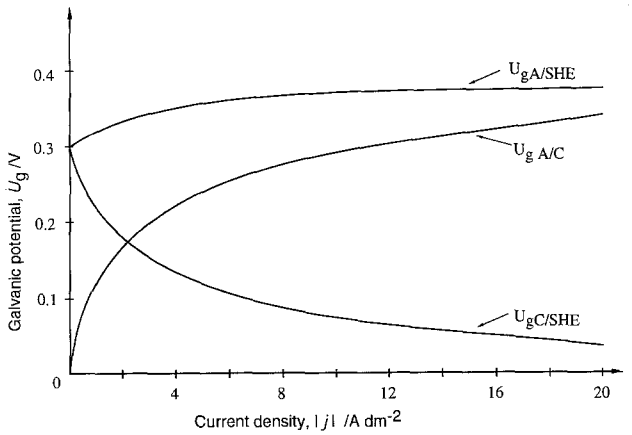

Fig. 12. Cathodic, anodic and anode to cathode polarization curves for copper electrorefining. Cu coated Pt r.d.e; $\omega = 3000$ r.p.m.

voltage $U_{A/C} = 0.310$ V; solution resistivity = 3.2 Ω cm; $\alpha = 0.335$ radian; and $U_{gA/C}(V) = 0.12 + 0.17 \log j$ (from Fig. 12 for $1 < j < 20$ A dm^{-2}).

These conditions give a value of the Wagner number $Wa = 0.9$. Figure 7 shows that the metal distribution (j_{exp}) and the secondary current distribution (j_{sec}) are very similar. Due to the polarization effect, the experimental ratio j_{max}/j_{min} is equal to 2.2

Example 2: Copper electrorefining at an electrolyte velocity of 0.2 m s^{-1}, high mean current density (8.1 A dm^{-2}) and high value of j/j_{dl} (Fig. 8).

The same data as above are used except for the cell voltage: $U_{A/C} = 0.845$ V. Wa is then 0.22. Figure 9 shows that the metal distribution deviates from the secondary current distribution at the highest current densities due to the increasing effect of mass transfer.

This deviation does not result from the model but from kinetic data. The polarization curves in Fig. 12 have been plotted for a rotation speed of 3000 r.p.m. The diffusion limiting current density is thus very high and the cathodic polarization curve does not contain any diffusion overvoltage. The anode to cathode galvanic potential is thus underestimated at high current density. To obtain kinetic measurements, taking into account the same mass transfer as in the modified Hull cell, polarization curves should be plotted on a r.d.e. at a rotation speed giving the same diffusion limiting current density as in the modified Hull cell. However, for high metal concentrations in agitated solutions, at current densities approaching 60% of j_{dl}, the amount of electricity passed through the cell is so high that enough metal is deposited at the r.d.e. to achieve a significant and continuous increase in roughness of the deposit, resulting in hydrodynamic perturbations and erratic results. It would be necessary to study this electrochemical system in a flow through rectangular channel cell where the current distribution is constant after the entrance effect with an electrolyte velocity providing the same j_{dl} as in the modified Hull cell; these types of measurements are beyond the scope of this paper.

Example 3: Copper electrorefining at an electrolyte velocity of 0.7 m s^{-1}, high mean current density (9.8 A dm^{-2}) but relatively low value of j/j_{dl} (Fig. 9).

The same data as above are used with a cell voltage $U_{A/C} = 0.98$ V, Wa of 0.18. In this case, the anode to cathode galvanic potential is not underestimated and the experimental metal distribution is identical to the secondary current distribution; the model is well adapted. Figure 9 shows also that metal distribution is very close to the primary current distribution; the solution resistivity has an overwhelming influence at high current densities.

(b) *Copper electrowinning*

Here oxygen evolution occurs at the lead anode. This permits study of the effect of the anodic polarization on the metal distribution on the cathode. The anode to cathode polarization curve (Fig. 13) is very flat with a high value of $U_{gA/C}$ over a large range of current density above 1 A dm^{-2}. This results in a more uniform cathodic metal distribution.

Results of copper electrowinning performed at an electrolyte velocity of 0.35 m s^{-1} and mean current density of 1.96 A dm^{-2} or 5.65 A dm^{-2} (Figs 10 and 11) show that the experimental metal distribution at low current density is very different from the primary current distribution. The experimental ratio j_{max}/j_{min} is below 2.1 and lower than that obtained under the same conditions in electrorefining. The Wa number is effectively higher than that calculated in electrorefining. An increase in the current density makes the metal distribution closer to the primary current distribution.

Plotted in Figs 10 and 11, the secondary current distribution is calculated with the following data: solution resistivity = 3.2 Ω cm; $\alpha = 0.335$ radian; $U_{gA/C}(V) = 2.38 + 0.19 \log j$ (from Fig. 17 for $1 < j < 20$ A dm^{-2}); and cell voltage $U_{A/C} = 2.2$ V for $j_{mean} = 1.96$ A dm^{-2} ($Wa = 1.00$) also $U_{A/C} = 2.55$ V for $j_{mean} = 5.65$ A dm^{-2} ($Wa = 0.35$). Results show that the calculated secondary metal distribution is in good agreement with the measured metal distribution.

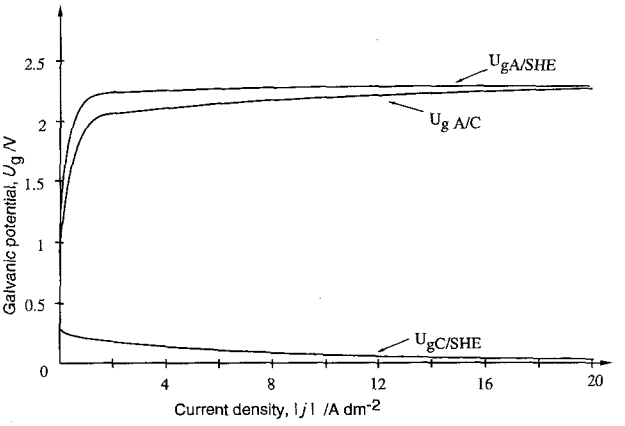

Fig. 13. Cathodic, anodic and anode to cathode polarization curves for copper electrowinning. Cathode: Cu coated Pt r.d.e; $\omega = 3000$ r.p.m. Anode: Pb.

4.2.2. Zinc electrowinning. Compared with copper electrowinning, an additional problem arises because the current efficiency is always below 100% and depends on the local current density.

To predict as exactly as possible the metal distribution, the primary current density for zinc, taking into account the local current efficiency, and the partial polarization curve for zinc deposition must be known. This means that the galvanic potential and the partial current density for zinc, based on deposit weight, must be measured point by point. This could be obtained by steady state measurements in a flow through rectangular channel cell with a speed of electrolyte providing the same j_{dl} as in the modified Hull cell taking into account the effect of hydrogen evolution at the local current density studied. A great number of deposits at different current densities must be carried out. Therefore, the zinc deposits study in the modified Hull cell would become unnecessary.

On the other hand, for a rapid study of the zinc deposit quality, an approximate primary zinc distribution may be satisfactory.

The primary current density for zinc can be estimated by two methods. The global zinc deposit weight gives the mean current efficiency and the mean partial current density for zinc. Two extreme situations may be considered.

(i) The local current efficiency equals the mean current efficiency; in this case, the partial current density for hydrogen evolution is proportional to the partial current density for zinc.
(ii) The partial current density for hydrogen evolution is constant along the cathode; the partial primary current density for zinc is then the difference between the global primary current density and the partial one for hydrogen.

The correct primary current density must lie between these two extremes. Experimental metal distribution obtained for zinc electrowinning at $0.2\,m\,s^{-1}$ and two different current densities (1.96 and $7.8\,A\,dm^{-2}$) was effectively found to be close to the primary current distribution calculated with a constant current efficiency along the cathode.

5. Conclusions

A new modified flow through Hull cell was designed, built and tested with copper and zinc deposition from acid baths.

Experiments showed that after a short entrance effect, mass transfer characterized by the diffusion limiting current density was constant on the cathode over a large range of turbulent flows, from 0.15 to $1.5\,m\,s^{-1}$. This cell can accordingly be used to simulate electroplating under industrial hydrodynamic conditions, especially for modern types of industrial cells where mass transfer is improved by circulation.

Except for edge effects at the inlet and outlet of the cathode, the current density is constant along the height of the electrode. A simple model based on the anode to cathode galvanic potential allows quantitative estimation of the metal distribution along the length of the cathode. Special attention must be paid to polarization measurements in the case of poor mass transfer and low current efficiency. The ratio of the maximum to minimum current densities studied in one experiment was low, ranging from 2.1 to 3.3. This cell is thus not very useful as a bath control cell where a large range of current densities is to be studied, but owing to its constant hydrodynamic conditions, this cell can be used to predict new industrial electroplating conditions directly transferable to the plant. Large area cathodes allow study of the influence of current density on the deposit structure.

Further developments currently under study are:

(i) enlarging the cross section of the cell by increasing the value of α and maintaining the same minimum distance between the two electrodes in order to increase the range of current densities studied during one experiment; to ensure hydrodynamic homogeneity some baffle plates placed in the adaptive channel may be needed;
(ii) modifying the electrolyte circuit in order to study laminar hydrodynamic conditions; specially designed baffles are necessary in this case;
(iii) increasing the height of the electrodes in order to decrease the relative influence of the upstream and downstream parts of the cathode;
(iv) studying other types of plating baths including more complex solutions.

References

[1] H. L. Pinkerton, 'Current and Metal Distribution' *in* 'Electroplating Engineering Handbook' (edited by L. J. Durney), 4th edn. Van Nostrand Reinhold, New York (1984) pp. 461–73.
[2] N. Ibl, *Surf. Technol.* **10** (1980) 81.
[3] Norm 50957 DIN, 'Galvanisierungsprüfung mit der Hull-Zelle', TAB 175, Beuth Verlag GmbH, Berlin and Köln (1983).
[4] M. Matlosz, C. Creton, C. Clerc and D. Landolt, *J. Electrochem. Soc.* **134** (1987) 3015.
[5] D. Pletcher and F. C. Walsh, 'Industrial Electrochemistry', 2nd edn., Chapman & Hall, London and New York (1990) pp. 389–91.
[6] R. H. Rousselot, *Metal Finish.* **57** (1959) 56.
[7] B. M. Luce, 'Current Distribution and Plating Tests' *in* 'Electroplaters' Process Control Handbook' (edited by D. G. Foulke) Robert E. Krieger, Huntington, New York (1975) pp. 113–32.
[8] R. Terakado and H. Nagasaka, *Metal Finish.* **77** (1979) 17.
[9] W. R. Parrish and J. Newman, *J. Electrochem. Soc.* **116** (1969) 169.
[10] *Idem, Ibid.* **117** (1970) 43.
[11] J. Newman, *ibid.* **113** (1966) 1235.
[12] R. V. Homsy and J. Newman, *ibid.* **121** (1974) 1448.
[13] H. M. Wang, S. F. Chen, T. J. O'Keefe, M. Degrez and R. Winand, *J. Appl. Electrochem.* **19** (1989) 174.
[14] A. Tvarusko and L. S. Watkins, *Electrochim. Acta* **14** (1969) 1109.
[15] *Idem, J. Electrochem. Soc.* **118** (1971) 580.
[16] M. Degrez and R. Winand, *Electrochim. Acta* **29** (1984) 365.
[17] D. J. Pickett, 'Mass Transfer Design Equations For Electrochemical Reactors' *in* 'Electrochemical Reactor Design' 2nd edn., Elsevier, Amsterdam and Oxford (1979) pp. 121–70.
[18] D. J. Pickett and K. Ong, *Electrochim. Acta* **19** (1974) 875.
[19] M. Degrez, A. A. Rodriguez Fajardo and R. Winand, *Oberfläche/Surface* **30** (1989-8) 20, (1989-9) 14.